Aalborg Universitet

Channel Estimation Using Spherical-wave Model for Indoor LoS and Obstructed LoS Scenarios

Yilin Ji, Wei Fan, Gert F. Pedersen,

Department of Electronic Systems, Faculty of Engineering and Science, Aalborg University, Denmark

Email: {yilin, wfa, gfp}@es.aau.dk

Abstract—**When the array apeture increases to a huge extent (e.g. tens to hundreds of wavelengths), and the distances between transmitter, scatterers, and receiver are small, conventional plane-wave model cannot be used to characterize the impinging wave accurately anymore. To avoid model mismatch during estimation, in this paper, we use spherical-wave model as the generic signal model, and estimate parameters of multipath component (MPC) with a maximum likelihood method for indoor line-of-sight (LoS) and Obstructed LoS (OLoS) scenarios. The estimated MPCs are reconstructed in the physical environment using a simple geometric method. Comparison with plane-wave model was also conducted to investigate the necessity of spherical-wave model.**

Index Terms—**Spherical-wave model, location of scatterer, near field, channel estimation.**

I. INTRODUCTION

Conventionally, the plane-wave signal model has been widely used to characterize multipath components (MPC) when transmit and receive arrays are small, and transmitter (Tx), scatterers, and receiver (Rx) are located far apart from each other. This is induced from the far-field assumption that the directions of impinging wave with respect to each antenna element are assumed to be parallel to each other. However, when array apeture increases to a huge extent (tens to hundreds of wavelengths), far-field assumption may not hold anymore. Therefore, a spherical-wave model [1], which approximates better the realistic propagation mechanism, should be used to avoid the model mismatch for channel estimation.

A model mismatch between plane-wave and spherical-wave model during channel estimation could lead to erroneous estimates of parameters, such as amplitude, and angle of arrival or departure of MPCs. The impact of the mismatch on different estimation algorithms does not vary, since it is essentially a signal model mismatch instead of an estimation algorithm flaw. However, this model mismatch would cause failure in some estimation algorithm. For specturm-based estimation algorithms like classic (Bartlett) beamforming, accuracy of angle estimate may remain acceptable, due to the robustness of this algorithm. In contrast, for maximum likelihood estimator which estimates parameters of each MPC in a successive interference cancellation (SIC) manner, the signal of estimated MPC cannot be cancelled from the whole signal, due to an inaccurate estimate of previous MPC. This would introduce artifacts into the original signal and makes the estimation of the rest MPCs unreliable.

In this paper, we processed the measurement data [2] which were measured in a regular-shape basement with a maximum likelihood algorithm. Two scenarios were considered, i.e. line-of-sight (LoS) and obstructed LoS (OLoS). A spherical-wave model was used as the generic signal model to estimate channel parameters, including amplitude, delay, azimuth of arrival (AoA), elevation of arrival (EoA), and the distance from scatterer to array. The MPC trajectories were reconstructed in the physical environment using a simple geometric method.

The rest of the paper is organized as follows. Section II describes the measurement campaign. Section III shows the estimation results of the parameters and comparison between plane-wave and spherical-wave model. Section IV introduced a method to map MPCs in physical environment. Section V concludes the paper.

II. MEASUREMENT CAMPAIGN

Fig. 1 shows the diagram of the measurement configuration and the photo of the measurement scene. The measurement were conducted in a regular shaped basement. Both the Tx and the Rx were equipped with an biconical omnidirectional antenna, respectively. The Tx and the Rx antenna are placed at the same height. The Rx antenna was fixed on an turntable, which enables rotation in the azimuth plane. A virtual uniform circular array (UCA) was formed by rotating the Rx antenna in 360° with 0.5° step and radius 0.5 m, corresponding to a virtual UCA of 720 elements. A vector network analyzer (VNA) was used to measure the channel frequency response from 28 GHz to 30 GHz with 750 frequency points for each UCA element position. The blackboard with metal substrate shown in Fig. 1 was used to produce the OLoS scenario. For the LoS scenario, the blackboard was removed from the environment. Walls are made of concrete. A detailed description of the measurement campaign can be found in [2].

III. RESULT ANALYSIS

In this section, two estimation algorithm have been applied to the measurement data, i.e. Bartlett beamforming and maximum likelihood estimator (MLE).

A. Results from a Bartlett Beamforming

The Bartlett beamforming has the advantages of robustness and low complexity. Here we use it to calculate the power delay-angle spectrum of the measured LoS and OLoS indoor
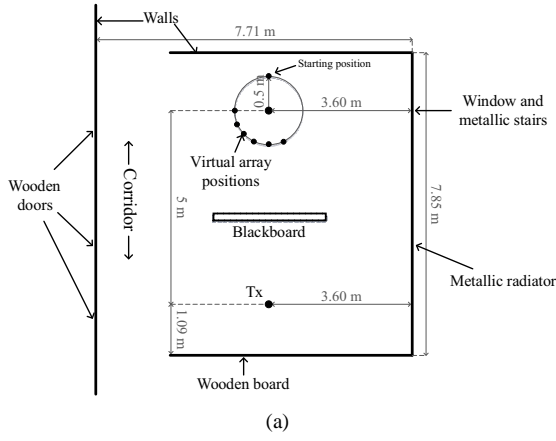
Fig. 1: (a) Diagram of the measurement configuration, and (b) photo of the measurement scene.
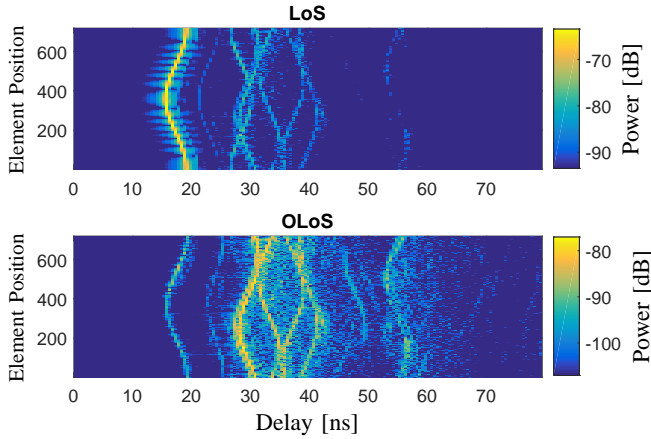

Fig. 3: Power delay-AoA specturm of the LoS case (top) and the OLoS case (bottom), calculated from Bartlett beamforming. EoA was set to $90°$ (i.e. azimuth plane); MPCs obtained from MLE shown in white circles.

Fig. 2: Measured CIR of the LoS case (top) and the OLoS case (bottom).
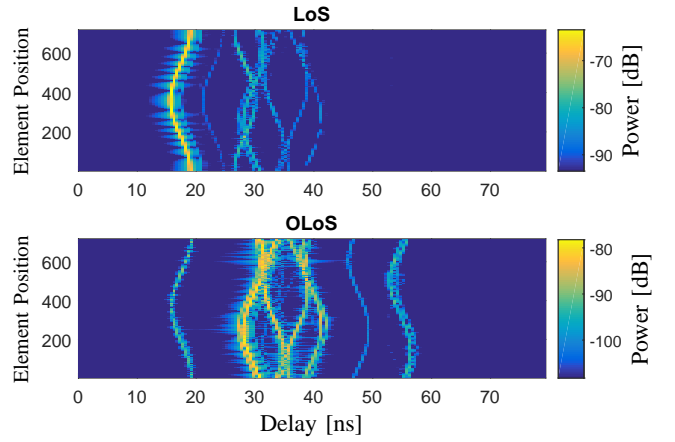
Fig. 4: Reconstructed CIR of the LoS case (top) and the OLoS case (bottom) from MLE estimation results.

channels. The plane-wave signal model was used as the array steering vector due to its simplicity.

Fig. 2 shows the channel impulse responses calculated by taking inverse fast fourier transform (IFFT) to the measured frequency responses for both the LoS and OLoS cases. It can be observed that due to the wide 2 GHz bandwidth, difference b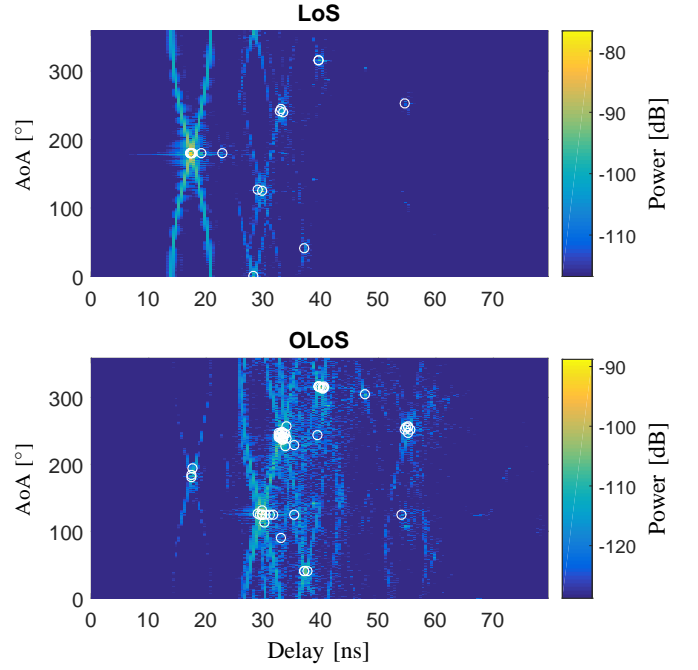etween propagation delay over antenna elements cannot be neglected, meaning the narrowband assumption [3] is not valid and array steering vector would be frequency dependent.

This can also be proved from Fig. 3 which shows the power delay-AoA spectum calculated from Bartlett beamforming for both cases. The "X"-shape power spectrum show exactly the frequency dependency of the array steering vector as reported in [2].

Fig. 5: Scheme of mapping MPCs to physical environment.

B. Results from a Maximum Likelihood Estimator

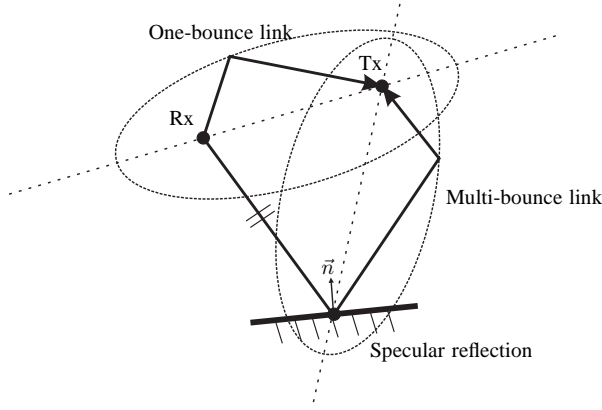The channel parameters including amplitude, delay, AoA, EoA, distance from scatterer to Rx of each MPC are estimated with spherical-wave model in a successive interference cancellation (SIC) way. The MPC of the highest likelihood is estimated first, and then the next MPC is estimated with the reconstructed signal of the previous MPC subtracted from the original measurement data. Totally 60 paths are assigned to the maximum likelihood estimator for the LoS and OLoS case, respectively.

Fig. 4 shows the reconstructed CIR from MLE estimation results for both the LoS and the OLoS cases. 30 dB dynamic range are used with respective to their strongest paths. After applying the power threshold, 20 and 59 paths are left for the LoS and OLoS cases, respectively. By comparing with the measured CIR shown in Fig. 2, a good comformity between the reconstructed CIR and measured CIR can be seen.

On top of the power delay-AoA spectrum shown in Fig. 3, we plot the estimated MPCs from MLE in delay-AoA domain (shown as white circles). It shows that the locations of peaks of the bartlett power spectrum match very well with the MLE results.

IV. MAPPING MPCs TO PHYSICAL ENVIRONMENT

Once the parameters of each MPC are estimated, it is straightforward to trace the propagation path in physical environment. The advantage of this physical mapping is that by visualizing the propagation path in physical environment, we can give a physical interpretation of the propagation mechanism of each MPC. However, since there is no sufficient geometric information for multi-bounce paths, the mapping could be inaccurate when the order of bounce increases.

The idea of this physical interpretation has been proposed in many literature [4]–[6], although some of them are implemented in different way. Fig. 5 shows the scheme of mapping MPCs to physical environment implemented in our case.
For one-bounce link: The location of the Tx and the Rx are regarded as the foci of an ellipse, and the size of the ellipse is determined by the product of delay and the speed of light.
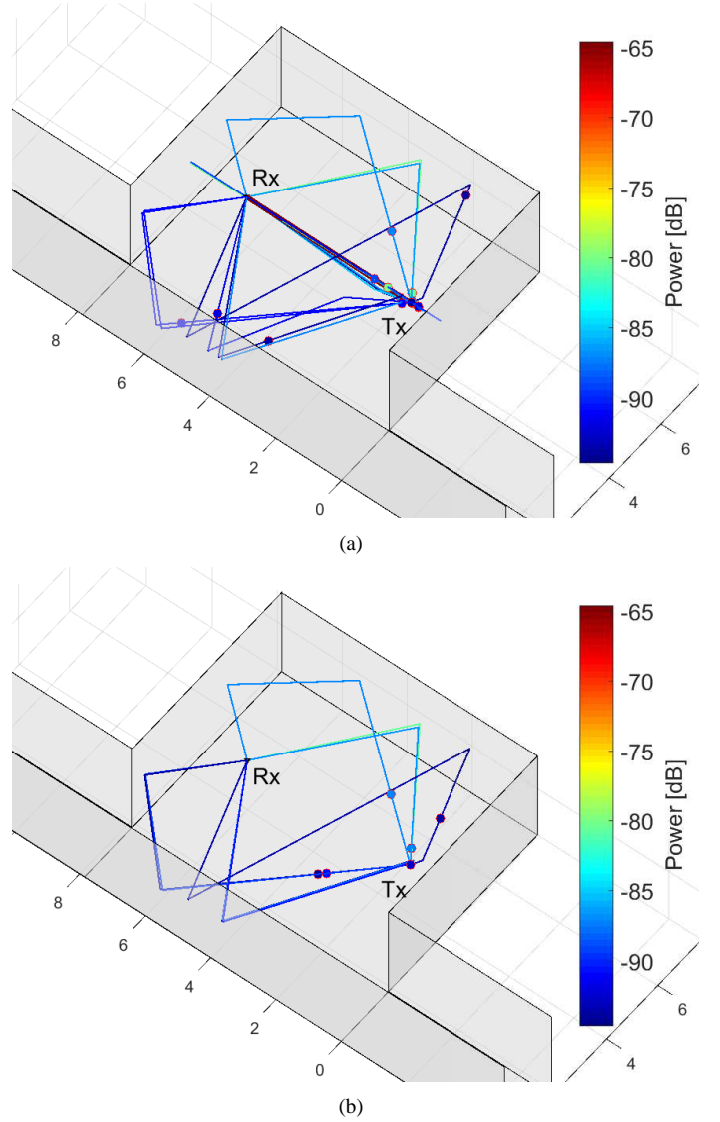

(a)

(b)

Fig. 6: The reconstructed MPCs in the physical environment for (a) the LoS case, and (b) the OLoS case. The same 30 dB dynamic range are considered for both cases. 20 and 9 paths are left, respectively.

Given the AoA and EoA, an MPC can be reconstructed in the 3D space uniquely.
For multi-bounce link: To avoid the resultant bouncing point located outside the measurement room, the map of the room is used, and walls are regarded as boundaries of the propagation environment. Moreover, specular refelection is assumed so that the reflection angle can be calculated with respect to the normal vector $\vec{n}$ of the walls. The propagation path of the last bounce is reconstructed as a one-bounce link.

The drawback of this implementation is that it only works for some simple environment without many scatterers inside. With a higher number of bouncing times, the assumption of specular reflection is less likely to be held. Fig. 6 shows the reconstructed MPCs in the measurement environment for both

the LoS and OLoS cases. The locations of scatterers are also plotted along the propagation paths since the distance from the scatterer to the Rx is estimated as a channel parameter with spherical-wave model. The locations of scatterers are represented with dots of red edge. It can be observed that for a regular-shape room without many scatterers inside, the reconstructed locations of scatterers tend to approach the location of the Tx.

V. CONCLUSION

In this paper, the measurement data obtained in a basement were processed with a maximum likelihood estimator. The spherical-wave model was used to estimate channel parameters. It was shown that the spherical-wave model gives a good representation of the MPCs when scatterers are located at the near field of array. A geometric mapping of MPCs to physical environment was also implemented.

REFERENCES

[1] T. Hirano and N. Kikuma, "Location Estimation of Multiple Near-Field Broadband Sources by Combined Use of DOA-Matrix Method and SAGE Algorithm in Array Antenna Processing," *Proceedings of ISAP2012, Nagoya, Japan*, pp. 363–366, 2012.

[2] W. Fan, I. Carton, J. Ø. Nielsen, K. Olesen, and G. F. Pedersen, "Measured wideband characteristics of indoor channels at centimetric and millimetric bands," *EURASIP Journal on Wireless Communications and Networking*, vol. 2016, no. 1, p. 58, 2016.

[3] H. Krim and M. Viberg, "Two decades of array signal processing research: the parametric approach," *IEEE Signal Processing Magazine*, vol. 13, pp. 67–94, 1996.

[4] B. Fleury, P. Jourdan, and a. Stucki, "High-resolution channel parameter estimation for MIMO applications using the SAGE algorithm," *2002 International Zurich Seminar on Broadband Communications Access - Transmission - Networking (Cat. No.02TH8599)*, pp. 30–1–30–9, 2002.

[5] G. Del Galdo, V. Algeier, N. Czink, and M. Haardt, "Spatial Localization of Scattering Objects from High-Resolution Parameter Estimates," *NEWCOM-ACORN Workshop, Vienna*, no. 1, pp. 1–21, 2006.

[6] J. Poutanen, K. Haneda, J. Salmi, V.-m. Kolmonen, A. Richter, P. Almers, and P. Vainikainen, "Development of measurement-based ray tracer for multi-link double directional propagation parameters," *Antennas and Propagation, 2009. EuCAP 2009. 3rd European Conference on*, pp. 2622–2626, 2009.